Hydrodynamic Force Measurements: Boundary Slip of Water on Hydrophilic Surfaces and Electrokinetic Effects

Elmar Bonaccurso, Michael Kappl, and Hans-Jürgen Butt*

Physikalische Chemie II, Universität Siegen, 57068 Siegen, Germany

(Received 11 June 2001; published 1 February 2002)

The hydrodynamic drainage force of aqueous medium between smooth hydrophilic surfaces was measured with the colloidal probe technique up to shear rates of typically 10^4 s^{-1}. Measured force curves were compared to simulations. To reach agreement between experimental and simulated force curves, the hydrodynamic force had to be fitted with a model allowing for boundary slippage. Boundary slip was characterized by a slip length of 8–9 nm. Force measurements with charged surfaces could be simulated taking only hydrodynamic and electrostatic double-layer forces into account.

DOI: 10.1103/PhysRevLett.88.076103 PACS numbers: 68.08.De, 47.20.–k, 68.37.Ps, 82.65.+r

The structure and mechanical properties of fluids at solid surfaces is important in many phenomena such as lubrication, adhesion, wetting, colloidal hydrodynamics, and microfluidics. In fluid mechanics, one usually relies on the assumption that, when liquid flows over a solid surface, the liquid molecules adjacent to the solid are stationary relative to the solid and that the viscosity is equal to the bulk viscosity. Though this might be a good assumption for macroscopic systems, it is questionable at molecular dimensions. Measurements with the surface forces apparatus (SFA) [1–3] and computer simulations [4–6] showed that the viscosity of simple liquids can increase by many orders of magnitude, or even undergo a liquid-to-solid transition, when they are confined between solid walls separated only few molecular diameters. Several experiments indicated that also isolated solid surfaces induce a layering in an adjacent liquid and that the mechanical properties of the first molecular layers are different from the bulk properties [7–10]. The change in the mechanical properties can be characterized by the position of the plane of shear. Simple liquids often show a shear plane which is typically 3–5 molecular diameters away from the solid-liquid interface.

Most of the experiments have been done for wetting fluids. For nonwetting fluids slippage was observed [11–14]. Computer simulation confirmed that for low fluid-wall interactions slippage occurs [15–17]. The hydrodynamic boundary condition to describe slippage is [18] $v_S = b d v_x/dz$. Here, v_S is the slip velocity, $d v_x/dz$ is the local shear rate, and b is the slip length. The slip length is the distance behind the interface at which the liquid velocity extrapolates to zero. There are, however, exceptions: Pit *et al.* observed slip with hexadecane on wetted sapphire surfaces [19]. Craig *et al.* inferred slip from force measurements with partially hydrophilic surfaces (advancing contact angle 70°) in aqueous sucrose solutions [20].

In this paper, we describe results of hydrodynamic force measurements between hydrophilic surfaces (mica and glass) in an aqueous medium using the colloidal probe technique. The hydrodynamic force depends critically on the boundary condition between the liquid and the solid surfaces. Thus, by fitting measured force-versus-distance curves (from now on called "force curves") with appropriate models, the boundary condition could be inferred. Significant slip was found for water even on hydrophilic surfaces.

Another purpose of this study was to check for electrokinetic effects in force measurements. Electrokinetic effects arise when a polar liquid flows over a charged solid surface. When dealing with particles, the shear of the liquid at charged surfaces leads to electroviscous forces [21]. Electroviscous forces were measured directly as a lift force acting on a particle moving parallel to a charged flat surface [22]. In force measurements with the colloidal probe technique, the particle approaches a wall in a normal direction. The liquid is drained out of the closing gap. Depending on the approaching velocity, high shear rates can occur. This might lead to an "electrokinetic effect" in the sense that the effective viscosity in the electric double layer increases [23].

To detect electrokinetic effects three types of experiments were done.

(i) "Hydrodynamic" force curves F_{hy} were recorded with high approaching velocities. High salt concentrations (200 mM monovalent salt, pH 5) were used so that the electrostatic double-layer force was negligible. Therefore, for distances $h > 2$ nm, the total interaction was purely hydrodynamic.

(ii) "Electrostatic" force curves F_{es} were recorded at low approaching velocity (negligible hydrodynamic force) in 2 mM monovalent salt and a pH around 11. Under these conditions, the electrostatic double-layer force dominates since the surfaces of borosilicate glass and mica are negatively charged and the Debye length is large (6.8 nm).

(iii) "Electrokinetic" force curves F_{ek} were recorded at high approaching velocities and a strong electric force (2 mM monovalent salt, pH 11). Electrokinetic force curves were compared to simulated force curves, taking the electrostatic double-layer force and the hydrodynamic force into account.

All experiments were done with the particle interaction apparatus which was described previously [24]. Spherical borosilicate glass particles (Duke Scientific Corporation, Palo Alto, California) were sintered to atomic force microscope (AFM) cantilevers. We used particles with radii $R = 10\ \mu$m to avoid an influence of the cantilever on the distance-dependent hydrodynamic force [25]. Rectangular cantilevers (length $L = 210\ \mu$m, width $w = 52.5\ \mu$m) made of silicon dioxide (1.0 μm thick, spring constant $K \approx 0.056$ N/m) and polycrystalline silicon (0.5 μm thick, $K \approx 0.012$ N/m) were specifically designed and produced (IMM, Germany). Spring constants of cantilevers were calibrated according to Sader *et al.* [26]. To measure force curves, a particle was positioned a few μm above the mica surface in a Teflon cuvette which was filled with aqueous electrolyte. Then the mica surface was periodically moved up and down at constant velocity ν_0 with a 12 μm range piezoelectric translator (Physik Instrumente, Germany, integrated position sensors, maximal ν_0: 70 μm/s). The deflection of the cantilever was measured with an optical lever technique. Therefore, light of a laser diode was passed through a waveguide (to obtain a rotational symmetric spot) and focused onto the back of the cantilever. The position of the reflected laser spot is measured with a position sensitive device (United Detectors, UK, active area 30×30 mm^2). Cantilever deflection was recorded as a function of piezo displacement. A force curve is calculated by multiplying cantilever deflection with the spring constant of the cantilever to obtain the force, and adding piezo displacement and cantilever deflection to obtain the distance from contact. The resolution is practically limited by the thermal noise of the cantilever, which in our case was below 0.3 nm, and the uncertainty in determining zero distance. Since the sample was hard compared to the stiffness of the cantilever the error in zero distance is probably negligible.

Two typical hydrodynamic force curves recorded at $\nu_0 = 4\ \mu$m/s and 40 μm/s are shown in Fig. 1. At high velocities even at large distances, the Stokes friction caused a deflection of the cantilever which did not depend on the distance. Stokes friction increased linearly with the velocity ν_0. When applying the Stokes equation of a sphere $F = 6\pi\eta R^* \nu_0$, we derive an effective radius R^* for the cantilever/particle of about 52 μm. Here, η is the viscosity of the liquid.

When the particle approaches the mica surface the repulsive force increases. This hydrodynamic distance-dependent repulsion increases with increasing approaching velocity. When retracting the particle with a low velocity, usually the particle adhered to the sample and an adhesion force had to be overcome. At high retracting velocities, a stronger apparent attraction is observed because an additional hydrodynamic force has to be overcome. Before the particle can retract, the liquid has to fill the widening gap between the particle and the flat surface.

We compared the experimental results with theoretical models. Calculations were first done with a no-slip condition which leads to a hydrodynamic force of [7,27] $F_{hy} = -6\pi\eta R^2/h \cdot dh/dt$. Here, dh/dt is the real velocity. In a second calculation, slippage was allowed by introducing a correction factor f^* according to Vinogradova [28]:

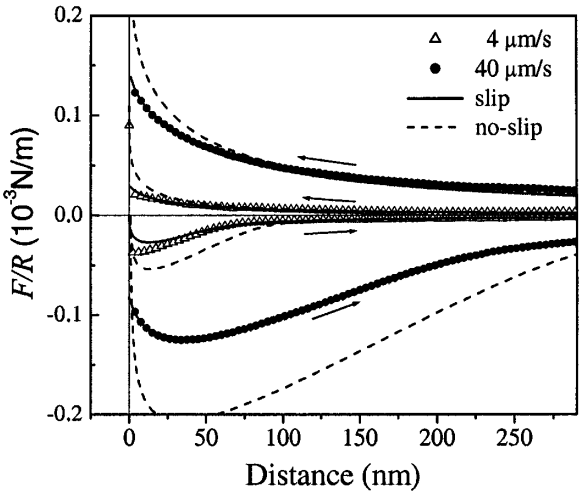

FIG. 1. Hydrodynamic force-versus-distance curves measured at low velocity ($\nu_0 = 4\ \mu$m/s, △) and high velocity ($\nu_0 = 40\ \mu$m/s, ●) in aqueous electrolyte (200 mM NaCl, pH 5) on mica. The force was normalized by dividing it by the radius of the glass particle $R = 10\ \mu$m. Only each 15th point is shown. Approaching and retracting parts of force curves are indicated by arrows. Simulations calculated according to Eq. (2) without ($f^* = 1$, dashed line) and with slip ($b = 8.6$ nm, continuous line) are plotted. Positive forces are repulsive; negative forces attractive.

$$F_{hy} = -\frac{6\pi\eta R^2}{h}\frac{dh}{dt} f^*$$
$$f^* = \frac{h}{3b}\left[\left(1 + \frac{h}{6b}\right)\ln\left(1 + \frac{6b}{h}\right) - 1\right]. \quad (1)$$

Both models assume creeping flow, Newtonian fluids, and small distances ($h \ll R$).

Hydrodynamic force curves were simulated by solving the equation of motion for a sphere moving towards a flat surface. Neglecting other surface forces, the hydrodynamic force is balanced by the restoring force of the cantilever; $F_K = K(h - h_0 + \nu_0 t)$. Here, h_0 is the initial separation at $t = 0$. The expression $h - h_0 + \nu_0 t$ is equal to the deflection of the cantilever. The effect of the hydrodynamic force is to retard the particle. As a consequence, the velocity of the particle at a given time t is not equal to ν_0 because the changing deflection of the cantilever has to be taken into account. This results in a nonuniform velocity of the particle during approach and retraction. The equation of motion, $F_h = F_K$, was calculated separately for the approaching and the retracting parts:

$$-\frac{6\pi\eta R^2}{h}\frac{dh}{dt} f^* = \begin{cases} K(h - h_0 + \nu_0 t) & \text{for approach} \\ K(h - h_r - \nu_0 t) & \text{for retraction.} \end{cases} \quad (2)$$

The position of the piezo at the beginning of the retraction was h_r. Equation (2) was solved numerically.

Force curves simulated with the no-slip boundary condition ($f^* = 1$) deviated significantly from measured force curves, especially at distances below 50 nm (Fig. 1). Even when introducing an additional prefactor to allow for possible inaccuracies in R or K, no agreement was achieved. When correcting for slip and simulating force curves with Eq. (2), calculations agreed with experimental force curves. Slip lengths of $b = 8-9$ nm were obtained independent of ν_0. We would like to point out that, except for the slip length, all parameters were determined independently.

The experimental results lead to the conclusion that boundary slip occurs for water on mica and/or glass. This opposes the current view about the structure and mechanical properties of water on hydrophilic surfaces. We do not have a good explanation and can discuss only possible hints for the discrepancy. The occurrence of a significant slip length does not necessarily imply slip on the molecular scale. It could also be a hint for a reduced viscosity. If the viscosity of the liquid in a surface layer of thickness δ is reduced from its bulk value η to η_S, the effective slip length is given by $b = \delta(\eta/\eta_S - 1)$. Previous experiments with the SFA [29,30] and flow measurements through thin capillaries [31] indicate that the bulk liquid viscosity is applicable down to separations below ten molecular diameters. Thus, we believe that a reduced viscosity is not the reason for slip.

Significant slip lengths of up to 20 nm were also found by Craig *et al.* in aqueous sucrose solutions (viscosities of 0.01–0.08 Pa s) [20]. They measured hydrodynamic forces between gold coated silica spheres and gold coated mica. The gold surfaces were coated with a self-assembled monolayer of alkanethiols leading to an advancing contact angle of 70°. In their case, slip lengths increased with increasing viscosity and shear rate. The aim of our study was (i) to avoid problems of gold/thiol coating such as the increased roughness, (ii) to use aqueous medium with its natural viscosity, and (iii) to use more hydrophilic surfaces.

Surface roughness could lead to an apparent slip length because in contact the liquid can still flow out of the gap beside the asperities. To exclude this, we imaged the particles with a commercial AFM in contact mode (Fig. 2). The roughness of the particles was below 1 nm rms. Peak-to-valley distances of areas of 1 μm^2 were below 2 nm.

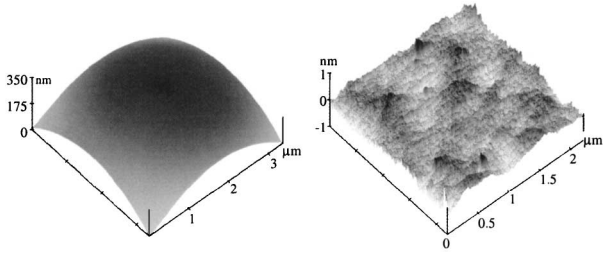

FIG. 2. AFM image of a glass particle recorded in contact mode using oxide-sharpened tips. The right figure was flattened and is shown at a height scale of 1 nm to show the roughness in detail.

Mica was atomically flat. Thus, surface roughness can probably not account for the slip lengths obtained. To verify that our surfaces were hydrophilic, the receding contact angle Θ_r of our glass particles was determined by microsphere tensiometry, where the interaction of the particle with an air bubble in an aqueous medium is measured [32]. We obtained zero contact angle. On mica also complete wetting was observed.

Why did we detect slippage, while in previous experiments no sign of slip was observed for water on smooth hydrophilic surfaces? One possible factor is the high shear rate we applied. For many liquids the viscosity depends on the shear rate [5,16,33], and experiments with partially wetted surfaces [14,20] indicate that the slip length increases with the shear rate. The maximal shear rate was calculated according to Horn *et al.* [13] taking into account that the velocity of the particle decreases from ν_0 at a large distance to zero for $h \to 0$. Typical maximal shear rates were 6000 s^{-1} for $\nu_0 = 20$ μm/s and 9500 s^{-1} for $\nu_0 = 40$ μm/s at a distance $h = 1$ nm.

Electrostatic force curves, recorded at low velocity at pH 11 and in 2 mM salt, showed the characteristic exponentially decaying double-layer repulsion. When fitting force curves with a constant charge model for the double-layer force decay lengths of 6.9 nm were obtained. This agrees with the calculated Debye length of $\lambda_D = 6.8$ nm. The constant potential model deviated at $h < 15$ nm from measured force curves.

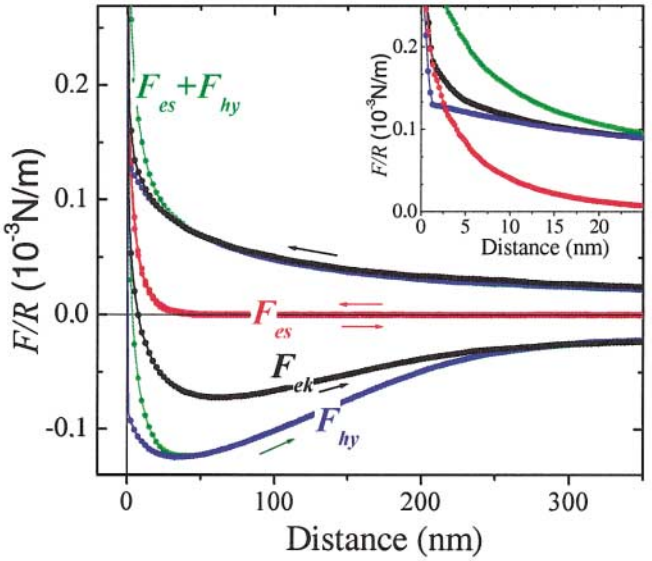

FIG. 3 (color). Normalized electrostatic F_{es} (red, $\nu_0 = 0.2$ μm/s, pH 11, 2 mM KOH) and electrokinetic force curve F_{ek} (black, $\nu_0 = 40$ μm/s, pH 11, 2 mM KOH). For comparison, also the hydrodynamic force F_{hy} (blue, $\nu_0 = 40$ μm/s, pH 5, 200 mM KCl) taken with the same particle ($R = 10$ μm) and cantilever is shown. In the range of the electric double layer, the sum of the electrostatic and hydrodynamic force, $F_{hy} + F_{es}$ (green), is higher than the electrokinetic force curve. Approaching and retracting forces curves are shown. The inset shows the approaching force curves in more detail. Only each 10th data point is shown.

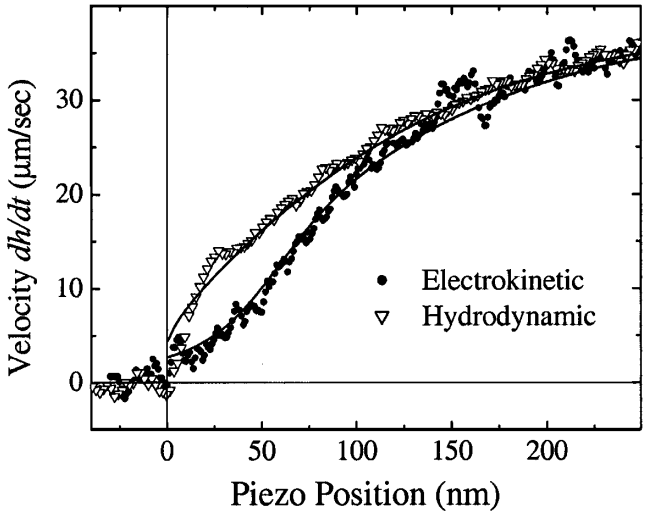

FIG. 4. Real velocity of the particle $|dh/dt|$ versus piezo position for a typical hydrodynamic ($\nu_0 = 40\ \mu$m/s, pH 5, 200 mM KCl, ∇) and an electrokinetic force curve ($\nu_0 = 40\ \mu$m/s, pH 11, 2 mM KCl, ●) recorded with the same particle. Continuous lines show results of simulations.

Electrokinetic force curves were more repulsive than electrostatic or hydrodynamic forces upon approach (Fig. 3). When retracting the particle, the electrostatic repulsion decreased the apparent hydrodynamic attractive force. The same results were obtained with NaCl, KCl, KOH, NaOH, and KI. Hence, the effect did not depend on the ion species. To simulate electrokinetic force curves, we took the hydrodynamic and double-layer forces into account. Therefore, a term Ae^{-h/λ_D} was added on the left side of Eq. (2). Here, A is the amplitude of the electrostatic double-layer repulsion. It was obtained by fitting electrostatic force curves for $h > 3$ nm with the constant charge model. Good agreement between simulated and experimental force curves was achieved even for the retracting part. We conclude that no special electrokinetic effect was present up to shear rates of typically $10^4\ s^{-1}$.

Electrokinetic force curves were less repulsive than the sum of the corresponding hydrodynamic and electrostatic force curves in the approaching part (Fig. 3): $F_{ek} < F_{hy} + F_{es}$. The reason is that when the particle approaches a charged surface and encounters an electrostatic repulsion its velocity $|dh/dt|$ decreases. The velocity in the presence of electrostatic repulsion is lower than without a double layer (Fig. 4). This reduces the hydrodynamic force and thus the total interaction.

We thank O. Vinogradova and G. Yakubov for helpful discussions. We further acknowledge financial support by the Deutsche Forschungsgemeinschaft grant Bu 701/14 (E. B.).

*Corresponding author.
Email address: butt@chemie.uni-siegen.de

[1] J. N. Israelachvili, P. M. McGuiggan, and H. M. Homola, Science **240**, 189 (1988).
[2] J. Van Alsten and S. Granick, Phys. Rev. Lett. **61**, 2570 (1988).
[3] J. Klein and E. Kumacheva, Science **269**, 816 (1995).
[4] M. Schoen, C. L. Rhykerd, D. J. Diestler, and J. H. Cushman, Science **245**, 1223 (1989).
[5] P. A. Thompson, G. S. Grest, and M. O. Robbins, Phys. Rev. Lett. **68**, 3448 (1992).
[6] J. Gao, W. D. Luedtke, and U. Landman, Phys. Rev. Lett. **79**, 705 (1997).
[7] D. Y. C. Chan and R. G. Horn, J. Chem. Phys. **83**, 5311 (1985).
[8] W. J. Huisman, J. F. Peters, M. J. Zwanenburg, S. A. de Vries, T. E. Derry, D. Abernathy, and J. F. van der Veen, Nature (London) **390**, 379 (1997).
[9] A. K. Doerr, M. Tolan, T. Seydel, and W. Press, Physica (Amsterdam) **248B**, 263 (1998).
[10] C. J. Yu, A. G. Richter, J. Kmetko, A. Datta, and P. Dutta, Europhys. Lett. **50**, 487 (2000).
[11] O. I. Vinogradova, Int. J. Miner. Process. **56**, 31 (1999).
[12] J. Baudry, E. Charlaix, A. Tonck, and D. Mazuyer, Langmuir **17**, 5232 (2001).
[13] R. G. Horn, O. I. Vinogradova, M. E. Mackay, and N. Phan-Thien, J. Chem. Phys. **112**, 6424 (2000).
[14] X. Zhu and S. Granick, Phys. Rev. Lett. **87**, 6105 (2001).
[15] M. Sun and C. Ebner, Phys. Rev. Lett. **69**, 3491 (1992).
[16] P. A. Thompson and S. M. Troian, Nature (London) **389**, 360 (1997).
[17] M. J. Stevens, M. Mondello, G. S. Grest, S. T. Cui, H. D. Cochran, and P. T. Cummings, J. Chem. Phys. **106**, 7303 (1997).
[18] P. G. de Gennes, C.R. Acad. Sci. B **288**, 219 (1979).
[19] R. Pit, H. Hervet, and L. Léger, Phys. Rev. Lett. **85**, 980 (2000).
[20] V. S. J. Craig, C. Neto, and D. R. M. Williams, Phys. Rev. Lett. **87**, 4504 (2001).
[21] P. Warszynski, Adv. Colloid Interface Sci. **84**, 47 (2000).
[22] S. G. Bike and D. C. Prieve, J. Colloid Interface Sci. **175**, 422 (1995).
[23] S. Levine, J. R. Marriott, and K. Robinson, J. Chem. Soc. Faraday Trans. 2 **71**, 1 (1975).
[24] S. Ecke, R. Raiteri, E. Bonaccurso, C. Reiner, H. J. Deiseroth, and H. J. Butt, Rev. Sci. Instrum. **72**, 4164 (2001).
[25] O. I. Vinogradova, H.-J. Butt, G. Yakubov, and F. Feuillebois, Rev. Sci. Instrum. **72**, 2330 (2000).
[26] J. E. Sader, J. Appl. Phys. **84**, 64 (1998).
[27] H. Brenner, Chem. Eng. Sci. **16**, 242 (1961).
[28] O. I. Vinogradova, Langmuir **11**, 2213 (1995).
[29] J. N. Israelachvili, J. Colloid Interface Sci. **110**, 263 (1986).
[30] U. Raviv, P. Laurat, and J. Klein, Nature (London) **413**, 51 (2001).
[31] N. V. Churaev, V. D. Sobolev, and A. N. Somov, J. Colloid Interface Sci. **97**, 574 (1984).
[32] S. Ecke, M. Preuss, and H.-J. Butt, J. Adhes. Sci. Technol. **13**, 1181 (1999).
[33] H. W. Hu, G. A. Carson, and S. Granick, Phys. Rev. Lett. **66**, 2758 (1991).